Article

A Spectroscopic and Electrochemical Approach to the Study of the Interactions and Photoinduced Electron Transfer between Catechol and Anatase Nanoparticles in Aqueous Solution

Teresa Lana-Villarreal, Antonio Rodes, Juan M. Prez, and Roberto Gmez

J. Am. Chem. Soc., **2005**, 127 (36), 12601-12611• DOI: 10.1021/ja052798y • Publication Date (Web): 17 August 2005

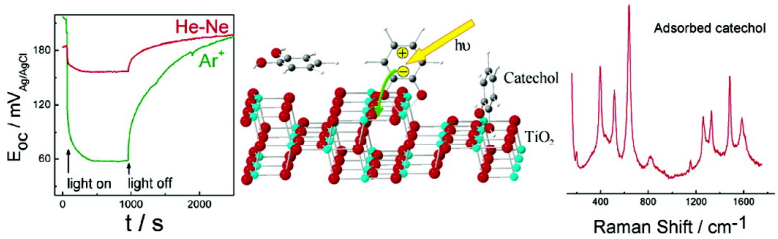

More About This Article

Additional resources and features associated with this article are available within the HTML version:

- Supporting Information
- Links to the 14 articles that cite this article, as of the time of this article download
- Access to high resolution figures
- Links to articles and content related to this article
- Copyright permission to reproduce figures and/or text from this article

View the Full Text HTML

J|A|C|S
ARTICLES
Published on Web 08/17/2005

A Spectroscopic and Electrochemical Approach to the Study of the Interactions and Photoinduced Electron Transfer between Catechol and Anatase Nanoparticles in Aqueous Solution

Teresa Lana-Villarreal, Antonio Rodes, Juan M. Pérez, and Roberto Gómez*

Contribution from the Departament de Química Física i Institut Universitari d'Electroquímica, Universitat d'Alacant, Apartat 99, E-03080, Alacant, Spain

Received April 29, 2005; E-mail: Roberto.Gomez@ua.es

Abstract: We have combined in situ photoelectrochemical and spectroscopic techniques (Attenuated Total Reflection Infrared, ATR-IR, and Resonance Raman Spectroscopy) for the study of the charge-transfer complex formed upon adsorption of catechol on anatase nanoparticles in contact with aqueous acidic solutions. Vibrational spectroscopies reveal the existence of at least two adsorbate configurations: catecholate in a chelate configuration and molecularly adsorbed catechol, with apparent ΔG°_{ads} values of -12.3 and -10.5 kJ mol^{-1}, respectively. These values are significantly less negative than the values reported for anatase colloidal dispersions. The adsorption of both catechol species on the nanoparticulate anatase thin films follows the Freundlich isotherm. As revealed by resonance Raman spectroscopy, only the adsorbed chelating catecholate forms the charge-transfer complex. The electron transfer from the adsorbate to the anatase nanoparticles has been evidenced by the development of a negative photopotential upon 514.5 or 632.8 nm laser illumination of an anatase nanostructured thin film electrode in contact with a catechol solution. The time evolution of the Raman spectra shows an increasing fluorescence indicating that, upon electron injection, catechol polymerization occurs on the TiO_2 surfaces. This conclusion is confirmed by in situ ATR-IR measurements, which show a progressive broadening of the catecholate bands together with the appearance of new signals. This study illustrates the benefits of combining electrochemical, infrared, and Raman techniques for the elucidation of processes occurring at the semiconductor/solution interface. Finally, evidence is given on the different adsorption and reactivity behavior found for suspensions and nanoporous thin films under equivalent experimental conditions.

1. Introduction

The past decade has witnessed an increased interest in the electrical, optical, and chemical properties of nanocrystalline semiconductor (SC) substrates.[1−5] For instance, the latter are critical for potential applications of nanocrystalline thin films in dye-sensitized photovoltaic cells[6] or in photocatalysis oriented to water purification.[7,8] More specifically, these applications require an in-depth knowledge of the electron-transfer processes occurring between SC nanoparticles and molecular adsorbates. Among all the SC oxides, titanium dioxide is the most studied one. It has been employed in practical devices due to its abundance and to its remarkable physical and chemical stability.

A number of articles have appeared on the surface modification of TiO_2 (mostly anatase nanoparticles) with adsorbates that form a surface charge-transfer complex, i.e., enediols, salicylic acid, etc.[9−20] Upon photoexcitation, an electron is considered to be transferred from the HOMO of the adsorbed molecule to the conduction band of the semiconductor, either directly or

(1) *Electrochemistry of Nanomaterials*; Hodes, G., Ed.; Wiley-VCH: Weinheim, 2001.
(2) *Semiconductor Nanocrystals: From Basic Principles to Applications*; Efros, A. L., Lockwood, D. J., Tsybeskov, L., Eds.; Kluwer Academic/Plenum Publishers: New York, 2003.
(3) *Chemical Physics of Nanostructured Semiconductors*; Kokorin, A. I., Bahnemann, D. W., Eds.; VSP BV: Zeist, 2003.
(4) *Semiconductor Nanostructures for Optoelectronic Applications*; Steiner, T., Ed.; Artech House: Norwood, 2004.
(5) *Encyclopedia of Nanoscience and Nanotechnology*, Nalwa, H. S., Ed.; American Scientific Publishers: Stevenson Ranch, 2004.
(6) *Encyclopedia of Electrochemistry, Vol. 6*; Bard, A. J., Stratmann, M., Eds.; Wiley-VCH: Weinheim, 2002.
(7) Hoffmann, M. R.; Martin, S. T.; Choi, W.; Bahnemann, D. W. *Chem. Rev.* **1995**, *95*, 69.
(8) Fujishima, A.; Tryk, D. A. In *Encyclopedia of Electrochemistry, Vol. 6, Semiconductor Electrodes and Photoelectrochemistry*; Bard, A. J., Stratmann, M., Eds.; Wiley-VCH: Weinheim, 2001.
(9) Moser, J.; Punchihewa, S.; Infelta, P. P.; Grätzel, M. *Langmuir* **1991**, *7*, 3012.
(10) Kratochvilová, K.; Hoskovcova, I.; Jirkovský, J.; Klíma, J.; Ludvík, J. *Electrochim. Acta* **1995**, *40*, 2603.
(11) Rodríguez, R.; Blesa, M. A.; Regazzoni, A. E. *J. Colloid Interface Sci.* **1996**, *177*, 122.
(12) Regazzoni, A. E.; Mandelbaum, P.; Matsuyoshi, M.; Schiller, S.; Bilmes, S. A.; Blesa, M. A. *Langmuir* **1998**, *14*, 868.
(13) Liu, Y.; Dadap, J. I.; Zimdars, D.; Eisenthal, K. B. *J. Phys. Chem. B* **1999**, *103*, 2480.
(14) Rajh, T.; Nedeljkovic, J. M.; Chen, L. X.; Poluektov, O.; Thurnauer, M. C. *J. Phys. Chem B* **1999**, *103*, 3515.
(15) Persson, P.; Bergström, R.; Lunell, S. *J. Phys. Chem. B* **2000**, *104*, 10348.
(16) Hao, E.; Anderson, N. A.; Ashbury, J. B.; Lian, T. *J. Phys. Chem. B* **2002**, *106*, 10191.
(17) Rajh, T.; Chen, L. X.; Lukas, K.; Liu, T.; Thurnauer, M. C.; Tiede, D. M. *J. Phys. Chem. B* **2002**, *106*, 10543.
(18) Wang, Y.; Hang, K.; Anderson, N. A.; Lian, T. *J. Phys. Chem. B* **2003**, *107*, 9434.
(19) Rego, L. G. C.; Batista, V. S. *J. Am. Chem. Soc.* **2003**, *125*, 7989.
(20) Redfern, P. C.; Zapol, P.; Curtiss, L. A.; Rajh, T.; Thurnauer, M. C. *J. Phys. Chem. B* **2003**, *107*, 11419.

indirectly, via the LUMO of the adsorbed molecule.[13−20] Apart from the intrinsic interest of these model systems for studying the electron-transfer process, these modifiers also act as surface photosensitizers, making the TiO_2 absorb and respond to visible light.[9−22] It is worth emphasizing that, in the case of catechol, the photosensitization does not seem to be conventional in that the modifier is excited in the visible wavelength regime, and the excited state injects an electron into TiO_2. In fact, most authors[14−18,20] consider that the modifier adsorption leads to the formation of an adsorbate-to-nanoparticle (ligand-to-metal) charge-transfer complex. What is photoexcited is this complex, leading to direct electron transfer from the modifier to the TiO_2 nanoparticle in a process sometimes known as photoinjection[15] as opposed to photosensitization. In addition, these adsorbates may also modify the rate of electron transfer to the surrounding aqueous solution or the rate of surface carrier recombination[9,22,23] because the surface states linked to electron traps (Ti(III)/Ti(IV)) could shift in some cases to the conduction band, changing drastically the lifetime of photogenerated electrons. These facts indicate that surface modification could be a practical way of tuning the photoelectrochemical properties of semiconductor nanoparticles.

Apart from the change in the Ultraviolet−visible (UV−vis) absorption spectrum of the SC, the effective existence of photoinduced charge transfer has been evidenced by means of transient absorption spectroscopy,[16,18] fluorescence quenching,[24−26] electron paramagnetic resonance,[14,17] and photocurrent measurements (see for instance ref 21).

Obviously, the phenomenon of surface sensitization involves the adsorption of an organic molecule (sensitizer) onto the semiconductor surface, i.e., the formation of a surface complex. Therefore, the determination of both adsorption sites and geometries is important in any description of the photochemistry and photophysics of these systems. In this respect, both theoretical ab initio methods and vibrational spectroscopic techniques may furnish valuable information.

One of the simplest molecules giving a surface charge-transfer complex when adsorbed on TiO_2 is catechol (1,2-dihydroxybenzene), which renders it a suitable choice as a model system.[9,11,13,15−20] In fact, a renewed interest in this system has arisen in the last years as evidenced by the appearance of a number of publications. In their pioneering work, Moser et al.[9] showed that the surface complexation of anatase with catechol increased by 2 orders of magnitude the rate constant for electron transfer from photoexcited TiO_2 to methyl viologen. Liu et al.[13] studied the interfacial charge-transfer complex in aqueous solution by Second-Harmonic Generation. Lian and co-workers[16,18] performed subpicosecond infrared−visible transient absorption experiments to characterize the dynamics of electron transfer between adsorbed catechol species and TiO_2 nanoparticles. Rajh et al.[14,17] studied the charge transfer triggered by photoexcitation of the surface complex by Electron Paramagnetic Resonance (EPR). Finally, several quantum mechanical calculations have appeared both on the interaction between TiO_2 and catechol (adsorption) and on the interfacial electron transfer.[15,18,19]

Surprisingly, there is a paucity of vibrational spectroscopic information on the interaction between catechol and anatase. Connor et al. presented preliminary results on the adsorption of catechol from alkaline solutions on TiO_2 obtained by means of Attenuated Total Reflection InfraRed (ATR-IR) spectroscopy.[27] A diffuse reflectance infrared spectrum from dried TiO_2 samples previously exposed to catechol-containing aqueous solutions has been also presented.[17]

As far as we know, no Raman study has been published on this system. As mentioned above, the formation of surface charge-transfer complexes leads commonly to sensitization to the visible. Thus, visible laser Raman spectroscopy arises as a convenient technique for studying these adsorbates because the laser probe photoexcites the charge-transfer complex, which leads to an enhancement of the Raman scattering phenomenon (Resonance Raman Scattering, RRS). In this respect, it is worth noting the thorough study done by Shoute and Loppnow on the adsorption of alizarin on a colloidal dispersion of TiO_2 nanoparticles.[28] These authors have studied not only the adsorption geometry but also the photoexcitation of the surface charge-transfer complex. In addition, we have applied very recently this technique to study the adsorption of salicylic and ascorbic acids on anatase nanoparticles.[29] Although less sensitive than infrared spectroscopy, two specific advantages of resonance Raman spectroscopy in this context should be mentioned: (i) no important interference from water is expected because of its low Raman cross-section; (ii) interference from solution species is suppressed since the resonance enhancement is restricted to the adsorbate (in the case of catechol and most of the simple surface complexing agents when dissolved in acidic solutions).

Finally, if catechol is adsorbed onto nanocrystalline anatase thin film electrodes, the charge-transfer process can be evidenced by photopotential measurements upon irradiation with visible light.

We would like to stress that the studies presented here also have implications in the field of photocatalysis. In fact, the photodegradation of catechol on TiO_2 has been studied repeatedly not only because this compound may be considered as a model contaminant[30,31] but also because it is an intermediate in the photocatalytic degradation of phenol.[32,33]

We present here for the first time a combined spectroscopic (Raman and infrared) and photoelectrochemical study on the surface charge-transfer complexation of anatase nanoparticles by catechol. This system is studied under both reactive and unreactive conditions. The existence of, at least, two different catechol adsorbates is concluded, although only one of them gives rise to the surface charge-transfer complex. In a more general vein, the fruitful combination of photoelectrochemistry

(21) Xagas, A. P.; Bernard, M. C.; Hugot-Le Goff, A.; Spyrellis, N.; Loizos, Z.; Falaras, P. *J. Photochem. Photobiol., A* **2000**, *132*, 115.
(22) Ramakrishna, G.; Ghosh, H. N. *Langmuir* **2003**, *19*, 505.
(23) Makarova, O. V.; Rajh, T.; Thurnauer, M. C.; Martin, A.; Kemme, P. A.; Cropek, D. *Environ. Sci. Technol.* **2000**, *34*, 4797.
(24) Itoh, K.; Chiyokawa, Y.; Nakao, M.; Honda, K. *J. Am. Chem. Soc.* **1984**, *106*, 1620.
(25) Hashimoto, K.; Hiramoto, M.; Lever, A. B. P.; Sakata, T. *J. Phys. Chem.* **1988**, *92*, 1016.
(26) Anz, S. J.; Krüger, O.; Lewis, N. S.; Gajewski, H. *J. Phys. Chem. B* **1998**, *102*, 5625.
(27) Connor, P. A.; Dobson, K. D.; McQuillan, A. J. *Langmuir* **1995**, *11*, 4193.
(28) Shoute, L. C. T.; Loppnow, G. R. *J. Chem. Phys.* **2002**, *117*, 842.
(29) Lana-Villarreal, T.; Pérez, J. M.; Gómez, R. *C. R. Chimie*, accepted.
(30) Hidaka, H.; Honjo, H.; Horikoshi, S.; Serpone, N. *New J. Chem.* **2003**, *27*, 1371.
(31) Peiró, A. M.; Ayllón, J. A.; Peral, J.; Domènech, X. *Appl. Catal. B* **2001**, *30*, 359.
(32) Azevedo, E. B.; Radler de Aquino Neto, F.; Dezotti, M. *Appl. Catal., B* **2004**, *54*, 165.
(33) Shchukin, D.; Poznyak, S.; Kulak, A.; Pichat, P. *J. Photochem. Photobiol., A* **2004**, *162*, 423.

and infrared and Raman spectroscopies applied to the SC/solution interface is highlighted.

This article is organized as follows. First, an infrared study on the dark adsorption of catechol at anatase nanoporous thin films is presented followed by a parallel Raman study for both anatase nanoporous thin films and slurries. The existence of two different adsorbates is evidenced together with information on their adsorption configurations. The comparison of corresponding infrared and Raman spectra allows one to identify which of the adsorbates yields the surface charge-transfer complex. Later both spectroscopies jointly with photopotential measurements are employed to monitor the charge separation and chemical reactivity processes.

2. Experimental Section

Chemicals and Materials. Nanocrystalline anatase TiO_2 particles (APS 32 nm) were purchased from Alfa-Aesar. Catechol (H_2cat) (Aldrich, 99+%), $HClO_4$ (Merck, p.a., 60%), and NaOH (Merck, p.a.) were used as received. All solutions were prepared using (Millipore Elix3) water with a conductivity of 18 $M\Omega^{-1}$ cm^{-1}. $(NH_4)_2[Ti(cat)_3]\cdot 2H_2O$ was synthesized following a published procedure.[34] $TiCl_4$ (Aldrich, 99.9%), HCl (Prolabo, Rectapur 35% min.), NH_4OH (Merck, p.a. 28−30%), NH_4Cl (Panreac, purissimum), KOH (Merck, p.a.), and ethanol (Prolabo, Normapur) were also used as received.

Infrared Spectroscopy. The ATR-IR experiments were carried out with a Nicolet Magna 850 spectrometer equipped with a MCT detector and a variable angle Veemax specular reflectance accessory (Pike Technologies). The ATR-IR cell was provided with a semicylindrical ZnSe window. Anatase films were coated onto the window by applying 0.4 μL mm^{-2} of a 0.4 M TiO_2 suspension and were dried in air overnight at 50 °C. The spectra were obtained by averaging 50 scans at a resolution of 8 cm^{-1} and at an angle of incidence of 45°. ATR-IR spectra of adsorbed catechol are presented as $-\log(R/R_o)$, where R_o corresponds to the single beam spectrum obtained for each TiO_2 film in the catechol-free 0.1 M $HClO_4$ solution. Solution spectra were recorded on the uncoated ZnSe prism. UV−vis irradiation of the TiO_2 film was carried out using a 50 W medium-pressure Hg lamp (PHYWE).

Ultraviolet−visible Absorption Spectroscopy. An anatase aqueous suspension (1% w/v) was sonicated for half an hour and allowed to stand for one week. Aliquots of 0.2 mL were added to 2 mL of 0.1 M $HClO_4$ or 0.1 M $HClO_4$ + 14.5 mM catechol. The corresponding diffuse transmission spectra were taken with a UV−vis spectrophotometer (UV-2401 PC Shimadzu) equipped with an integrating sphere (ISR-240A, Shimadzu).

Raman Spectroscopy. Raman spectra were obtained with a LabRam spectrometer (from Jobin-Yvon Horiba). The excitation line was provided by a 17 mW He−Ne (632.8 nm) or a 50 mW Ar^+ (514.5 nm) or a 100 mW diode laser (784.8 nm). The laser was focused through a 50× objective on the sample surface (slurry or thin film). The spectrometer resolution was better than 3 cm^{-1}, and the detector was a Peltier cooled charge-couple device (CCD). For Raman and photopotential experiments, the anatase thin films were prepared by electrophoresis from a TiO_2 suspension (1% w/v in methanol). A bias of 10 V was applied between the substrate (F-doped SnO_2, FTO, Asahi Glass Co, Japan) and a gold counter electrode for 60 s resulting in films with a thickness of approximately 3.5 μm. The films so formed were allowed to dry before thermal treatment at 450 °C for 1 h in air. The anatase slurries (0.16 g mL^{-1}) were placed for the Raman experiments in a thin layer cell (80 μm) equipped with a fused silica window.

(34) Borgias, B. A.; Cooper, S. R.; Koh, Y. B.; Raymond, K. N. *Inorg. Chem.* **1984**, *23*, 1009.

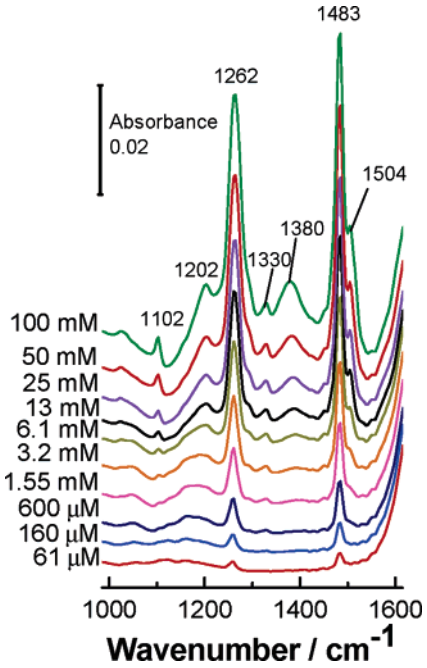

Figure 1. ATR-IR spectra for catechol adsorbed on anatase nanoporous films in contact with 0.1 M $HClO_4$ solutions containing different catechol concentrations (indicated alongside).

Photoelectrochemical Measurements. Photopotential measurements were performed using both a He−Ne (Melles Griot, 15 mW) and an Ar^+ (Ion Laser Technology, 110 mW) laser. The intensity of the incident light was measured with an optical power meter (Oriel model 70310), equipped with a thermopile head (Ophir Optronics 71964). Neutral density filters (Melles Griot) were used to obtain similar light intensities with both lasers. The open circuit potential was measured with a commercial computer-controlled potentiostat (Wenking POS2). A platinum wire was used as a counter electrode, and Ag/AgCl/KCl(sat), as a reference electrode. The electrolyte was purged with nitrogen before and during the experiments in order to remove dissolved oxygen.

3. Results and Discussion

3.1. ATR-IR Experiments without Photoexcitation. Figure 1 shows a series of spectra obtained for a nanoparticulate thin layer of anatase deposited on ZnSe and in contact with acidic solutions (0.1 M $HClO_4$) with concentrations of catechol ranging from 0.061 to 100 mM. The experiments have been done with catechol dissolved in 0.1 M $HClO_4$ because perchlorate anions are not expected to adsorb specifically. In this way, both ionic strength and solution pH can be adjusted without interference coming from supporting electrolyte adsorption. In addition, the adsorption of catechol is favored in acidic solutions.[11]

For catechol concentrations below 0.60 mM the spectra appear dominated by two bands at 1262 and 1483 cm^{-1} together with a less intense one that can be distinguished at around 1330 cm^{-1}. In this concentration range and in the absence of the anatase film, no bands for solution species can be distinguished, which allows us to ascribe the observed features to vibrations of species adsorbed on the anatase surface. Up to a concentration of 1.5 mM, the successive spectra do not show significant qualitative changes. The progressive increase in band intensity is linked to the increase in the amount of adsorbed substance. For catechol concentrations above 1.5 mM, new absorption bands develop at 1102, 1202, 1380, and 1504 cm^{-1} (see below). All the spectra are characterized by a broad band at around 1650

Table 1. Vibrational Frequencies for Catechol Adsorbed on TiO_2 Observed by Means of ATR-IR and RRS and Their Assignments[a]

adsorbate RRS ν/cm^{-1}	$(NH_4)_2[Ti(cat)_3]\cdot 2H_2O$ Raman ν/cm^{-1} solid	aqueous	adsorbate ATR-IR ν/cm^{-1}	$[Ti(cat)_3]^{2-}$(aq) IR ν/cm^{-1}	$catechol_{aq}$ pH = 1 IR ν/cm^{-1}	$catechol_{aq}$ pH = 13 IR ν/cm^{-1}	assignment	references
197, 396, 516, 637							TiO_2 lattice vibrations	46
			1102[b]	1099	1103	1099	δ(CH); δ(CH) + δ(OH)	36, 38
1155	1153, 1198			1207			δ(CH)	28, 36, 38
			1202[b]		1199	1224	δ(OH)	36, 37, 38
1261	1249, 1270	1250, 1265	1262	1245	1261, 1277	1257, 1284	ν(CO)	17, 28, 36, 37, 38
1329	1338	1336	1330	1330			ν(CO) + ν(CC)	28, 36, 38, 39
			1380[b]		1374	1358	δ(OH); δ(OH) + ν(CO) + ν(CC)	17, 36, 43
1483	1475, 1490	1484	1483	1477	1470	1489	ν(CC)	36, 37
			1504[b]		1516		ν(CC) + δ(CH)	36, 38
1584	1575	1580					ν(CO) + ν(CC)	28, 36, 38

[a] Infrared bands for catechol (pH = 1 and pH = 13) and $[Ti(cat)_3]^{2-}$ solutions (saturated) are also compiled as well as Raman bands for solid and aqueous (saturated solution) $(NH_4)_2[Ti(cat)_3]\cdot 2H_2O$. [b] Bands corresponding to the adsorbate appearing at high solution concentration.

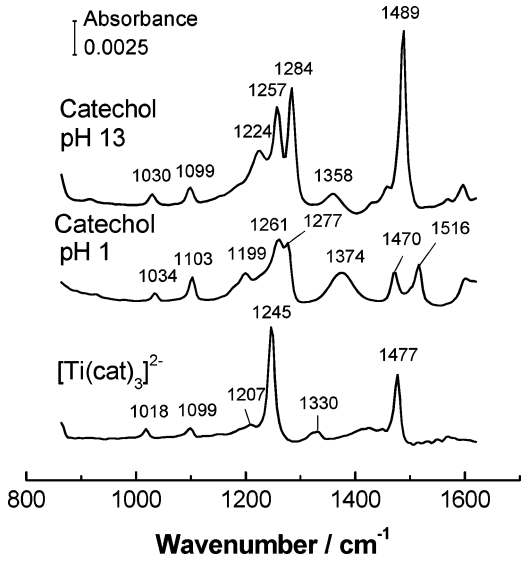

Figure 2. ATR-IR spectra for 0.1 M catechol aqueous solutions at pH 1 and 13 and for a saturated $(NH_4)_2[Ti(cat)_3]$ solution in 2 M NH_4Cl(aq). Interferograms (200) were collected and referred to a single beam spectrum collected in the absence of either catechol or the complex.

cm^{-1} (not shown) that can be related to infrared absorption from uncompensated water molecules.

Figure 2 shows catechol solution spectra (obtained by ATR-IR spectroscopy in the absence of the thin layer of nanoparticles) acquired at two different pH values: 1 and 13. The spectrum for a saturated $(NH_4)_2[Ti(cat)_3]\cdot 2H_2O$ aqueous solution is also given. It is worth noting at once that, despite the high concentration of catechol used, the intensity of the different features is significantly lower than that in the absence of nanoparticles. Large differences between the spectra for both catechol solutions can be observed, reflecting the pH-dependent speciation of catechol. While at pH 1 the protonated species predominates, at pH 13 there exists a mixture of both catecholates (half- and fully deprotonated) given that the pK_a's for catechol are 9.45 and 12.80.[35] The existence of the monoanion is clearly evidenced by the presence of a band at 1224 cm^{-1} attributed to a δ(OH) mode.[36] Unfortunately, due to the high value of pK_{a2} and to the instability of the strongly alkaline solutions of catechol, a spectrum corresponding mainly to catecholate (dianion) in solution could not be obtained. Nevertheless, the spectrum for the $[Ti(cat)_3]^{2-}$ complex shows the spectral signature for catechol bound to a Ti(IV) central ion. This is most informative as it is known that, in such a complex, the actual ligand is the dianionic catecholate species in a chelating configuration.[34] In any case, it is apparent that vibrational spectroscopy may be used as a diagnostic tool for identifying the nature of the adsorbate. A quick comparison of spectra for the adsorbate and catechol dissolved in alkaline solution suggests that catecholate is the adsorbed species formed on anatase at low and moderate concentrations of catechol in solution (below 1.5 mM) (see Table 1). In addition, the close resemblance of the spectrum for the complex with those shown in Figure 1 for the adsorbate in the low catechol concentration range indicates that the adsorbate probably adopts a chelating configuration.

It is of utmost importance to confirm the stoichiometry and configuration of the adsorbate at the surface of TiO_2. This can be achieved by a careful assignment of the bands appearing in the adsorbate spectrum. The band at 1483 cm^{-1} corresponds to one of the ν(CC) modes of the ring. It is significant that the infrared spectra of the anionic complexes $[Ti(cat)_3]^{2-}$ and $[TiO(cat)_2]_2^{2-}$, where the coordinated catechol is forming a deprotonated chelating species (bidentate mononuclear configuration), also show intense bands at 1477 (see Figure 2) and 1475 cm^{-1},[34] respectively. The band at 1262 cm^{-1} can be assigned quite confidently to a ν(CO) mode.[17,36−38] It is quite broad (32 cm^{-1} for the full width at half-maximum, fwhm), which could be linked to the fact that adsorption is most probably occurring through the phenoxy groups. In fact, the band corresponding to the same mode in the catechol alkaline solution (at 1257 cm^{-1}) is significantly narrower (fwhm = 15

(35) Oess, A.; Cheshire, M. V.; McPhail, D. B.; Stoll, S.; El Alaili, M.; Vedy, J. C. *Sci. Total Environ.* **1999**, *228*, 49.
(36) Greaves, S. J.; Griffith, W. P. *Spectrochim. Acta A* **1991**, *47*, 133.
(37) Martin, S. T.; Kesselman, J. M.; Park, D. S.; Lewis, N. S.; Hoffmann, M. R. *Environ. Sci. Technol.* **1996**, *30*, 2535.
(38) Öhrström, L.; Michaud-Soret, I. *J. Phys. Chem. A* **1999**, *103*, 256.

Scheme 1. Proposed Adsorbate Configurations: Chelate (left) and Molecularly Adsorbed (right)

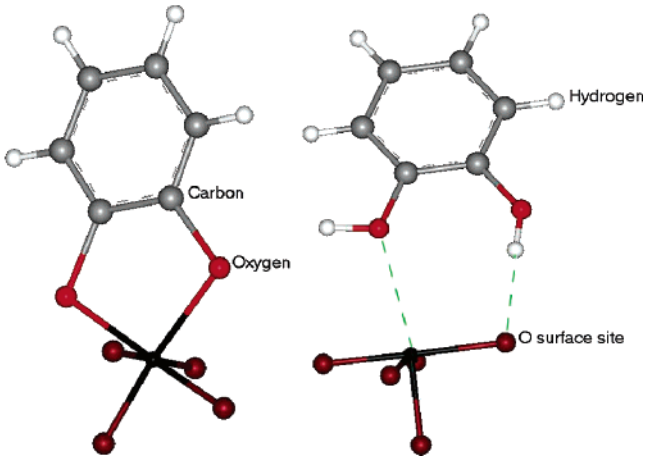

cm^{-1}). Remarkably, the spectra of $[Ti(cat)_3]^{2-}$ and $[TiO(cat)_2]_2^{2-}$ also show bands associated to the C−O stretching mode at 1245 (Figure 2) and 1249 cm^{-1},[34] respectively.

On the other hand, the weaker band at 1330 cm^{-1} has been ascribed to a combination of CO and ring stretches.[28,39] It also appears in the complexes mentioned above,[34] which rules out an assignment to δ(OH). Finally, it is worth mentioning that analogous bands at 1258, 1333, and 1481 cm^{-1} appear in the infrared spectrum for catecholate adsorbed on TiO_2 from strongly alkaline solutions (0.1 M NaOH).[27] Putting together all these pieces of information allows us to strongly suggest that the geometry for adsorbed catechol is akin to that in the complexes; i.e., both oxygen atoms of the catecholate species bind a Ti(IV) surface site, forming a chelate with a five-atom ring (see Scheme 1). The alternative bridging structure (bidentate binuclear) for the adsorbed catechol (dissociatively adsorbed at two Ti sites) does not seem to be energetically favored.[20]

The formation of a chelate species upon adsorption can only be explained if each Ti surface site has two dangling bonds available for adsorbates, as one catecholate species would saturate both of them. In bulk anatase the Ti atoms have a 6-fold coordination, but the coordination index lowers at the surface. In commercial anatase nanopowders, as the ones used in this study, a multiplicity of faces will be found. According to surface energy values, the (101) surface should be the most abundant one, followed by the (100) and (001) planes.[40] These surfaces are not expected to have 4-fold coordinated surface atoms (Ti(4)), but such a type of surface sites appears in typical reconstructions of the (001) surface. More importantly, the step edges appearing at the (101) surface are formed by Ti(4) atoms.[40,41] Therefore, the surface of our samples is expected to have a significant proportion of Ti(4) sites, especially considering that we are dealing with nanoparticles, whose proportion of surface defects (for instance, steps) is much larger than that for macroscopic crystals. Another point that should be stressed is that these unsaturated Ti surface sites show an increased avidity for adsorbates.[40,41] We can explain then both the formation of chelating species at the different sites where Ti surface atoms are four-fold coordinated and the predominance of this adsorbate for low concentrations of catechol in solution. The formation of these chelating adsorbates on TiO_2 has been suggested previously by Rajh et al.[14,17] Furthermore, a recent publication reporting computational studies for the adsorption of catechol on TiO_2 has evidenced that adsorption at defect Ti sites (four-fold coordinated) is favored over dissociative monodentate or molecular catechol adsorption.[20] Incidentally, the catechol chelating coordination mode is by far the most common one. It accounts for around 85% of the coordination compounds of catechol with metals.[42]

Figure 1 also shows that new adsorbate bands appear upon increasing the concentration of catechol in solution. This indicates that, once the Ti(4) adsorption sites are saturated, the 5-fold Ti(5) sites together with neighboring oxygen sites could serve to anchor adsorbed molecules. As mentioned above, new vibrational bands appear at 1102, 1202, 1380, and 1504 cm^{-1} (see Table 1). The first of them can be safely assigned to δ(CH) modes,[36] although interestingly, it has also been assigned to a combination band: δ(CH) + δ(OH).[38] The assignment of the bands at 1202 and 1380 is crucial in the present context. According to different authors these bands correspond to δ(OH) modes. In fact, Greaves and Griffith have assigned a band at 1353 cm^{-1} for catechol in acetonitrile solution to the OH deformation.[36] McBride and Wesselink assigned a band for free catechol at 1370 cm^{-1} to a C−C ring stretch coupled to an OH bend and to a C−O stretch.[43] Finally, Rajh has attributed a band appearing in the infrared spectra for dried catechol at 1365 cm^{-1} to a δ(OH) mode.[17] In the same way, the band at 1202 cm^{-1} has been also assigned to a δ(OH) mode by several authors.[36,37,38] The band at 1504 cm^{-1} has been attributed to a combination ν(CC) + δ(CH), typical of free, undissociated catechol.[36,38] Significantly, in the $[TiO(cat)_2]_2^{2-}$ complex no bands around these frequencies appear.[34] Admittedly, a weak band at 1207 cm^{-1} appears in the $[Ti(cat)_3]^{2-}$ spectrum, which in this case should be ascribed to a δ(CH) mode.[38] In the spectrum for acidic solutions of catechol, broad bands appear at 1199 and 1374 cm^{-1} whereas they are absent in the spectrum corresponding to alkaline solutions (Figure 2). Therefore, we can identify the second adsorbate as molecularly adsorbed catechol. In this adsorption geometry,[20] a hydrogen bond would be established between the H atom of one of the OH catechol groups and one of the O surface sites. Likewise, a van der Waals bond would be established between a Ti(5) site (typical of the most stable terraces) and the O atom of the other OH group of catechol (see Scheme 1). Alternatively, instead of the Ti/O van der Waals bond, another hydrogen bond could be established between the O atom of the second OH group and the H atom of a hydroxide anion/water molecule adsorbed on the Ti site.

The possibility of dissociative monodentate adsorption should be also envisaged. In such an adsorption mode, one of the catechol OH groups would be dissociated and directly bonded to the Ti site, and the other, undissociated, would interact via a hydrogen bond with an adjacent oxygen surface site. The calculated adsorption energies for dissociative monodentate and molecular configurations are similar.[20] However, the spectral behavior described above points to the prevalence of molecular adsorption. The spectrum for the catecholate monoanion shows

(39) Sánchez-Cortés, S.; García-Ramos, J. V. *J. Colloid Inteface Sci.* **2000**, *231*, 98.
(40) Diebold, U. *Surf. Sci. Rep.* **2003**, *48*, 53.
(41) Hebenstreit, W.; Ruzycki, N.; Herman, G. S.; Gao, Y.; Diebold, U. *Phys. Rev. B* **2000**, *62*, R16334.
(42) Gigant, K.; Rammal, A.; Henry, M. *J. Am. Chem. Soc.* **2001**, *123*, 11632.
(43) McBride, M. B.; Wesselink, L. G. *Environ. Sci. Technol.* **1988**, *22*, 703.

a band for the OH bend at 1225 cm^{-1} as indicated by Greaves and Griffith.[36] This band (at 1224 cm^{-1}) also appears in our spectrum for the catechol solution at pH = 13, which contains both the monoanion and the dianion, but it does not appear in the spectrum for the second adsorbate. In addition, the spectrum for the dianion does not show a band at 1504 cm^{-1},[36] nor does this band appear in the infrared spectrum of a Ti complex with 3,5-di-*tert*-butylcatechol, which contains monohydrogenated ligands.[34]

As can be deduced directly from Figure 1, the coverage of both adspecies does not grow in a parallel way; i.e., the ratio between the absorbances of two bands corresponding to each of them is not constant. This indicates that the adsorption is noncompetitive. Thus, the adsorption of catechol occurs forming two adspecies that do not compete for the same sites. The most favorable configuration corresponds to a chelating species adsorbed at Ti(4) defect sites whereas the second one corresponds to catechol molecularly adsorbed and interacting both with a Ti(5) site and with an adjacent oxygen site (see Scheme 1). The existence of two different adspecies resulting from the adsorption of catechol on TiO_2 was postulated in a previous study dealing with the determination of adsorption isotherms.[11]

3.2. Adsorption Isotherms and Energy of Adsorption. The ATR-IR experiments may be used to determine adsorption isotherms as demonstrated previously.[44] We deal with each of the adsorbates separately. This is achieved by deconvoluting in the experimental spectra the bands at 1483 and 1504 cm^{-1} and assuming that the coverage (θ) is proportional to the integrated absorbance (Abs), that is, $\theta_{cat} \alpha Abs_{1483}$ and $\theta_{H_2cat} \alpha Abs_{1504}$. Figure 3A shows the Abs vs catechol concentration plots for both adspecies.

The Freundlich isotherm (Figure 3B) fits these data better than the Langmuir one. This is understandable, as the Freundlich isotherm has been shown to result from a variant of the Langmuir derivation but taking into account a continuous distribution of adsorption heats. In a highly heterogeneous sample as the one we are using here, a variety of adsorption sites with different adsorption energies is expected to exist (within each of the Ti(4) and Ti(5) surface coordinations). Nonetheless, it is noteworthy that in previous works the Langmuir isotherm could account reasonably for the experimental behavior.[9,11,13] From Langmuirian plots (not shown), approximate values for the apparent standard Gibbs adsorption energy can be calculated (molar scale). A value of −12.3 kJ mol^{-1} can be obtained for the catecholate adspecies whereas a value of −10.5 kJ mol^{-1} is found for molecularly adsorbed catechol. Previous estimates for ΔG°_{ads} yielded significantly more negative values ranging from −28 kJ mol^{-1} to −38 kJ mol^{-1}.[9,11,13] The main differences between those experiments and the ones reported here are the pH value (lower in our case) and the type of nanoparticulate samples used: whereas we are using a nanoparticulate thin film, the other studies were performed with colloidal dispersions. According to the results obtained by Rodríguez et al.,[11] the pH value does not seem to exert an important effect on the adsorption isotherm as long as it is lower than 9. Recently, Morand et al.[45] have suggested, on the basis of Quartz Microbalance measurements, that the adsorption of benzoic acids is accompanied by an important displacement of water from the pores of the nanoparticulate film. They attributed this behavior to the hydrophobicity imparted to the TiO_2 surface by the adsorbate. The significantly lower adsorption Gibbs energy found in our case compared to nanoparticle dispersions is probably linked to the fact that the work of extraction of water from the pores should be added to the intrinsic (negative) value of ΔG°_{ads} for catechol. In a more general vein, our observation together with those by Morand et al.[45] suggests that the behavior of nanostructured electrodes could differ significantly from that found in colloidal dispersions of the particles forming the thin film. Concretely, the pores in the film may become highly hydrophobic, which could induce an inner solution composition significantly different from that in the solution bulk. This, of course, would have important consequences in the photoreactivity of these nanostructures. More work is needed to further substantiate these ideas.

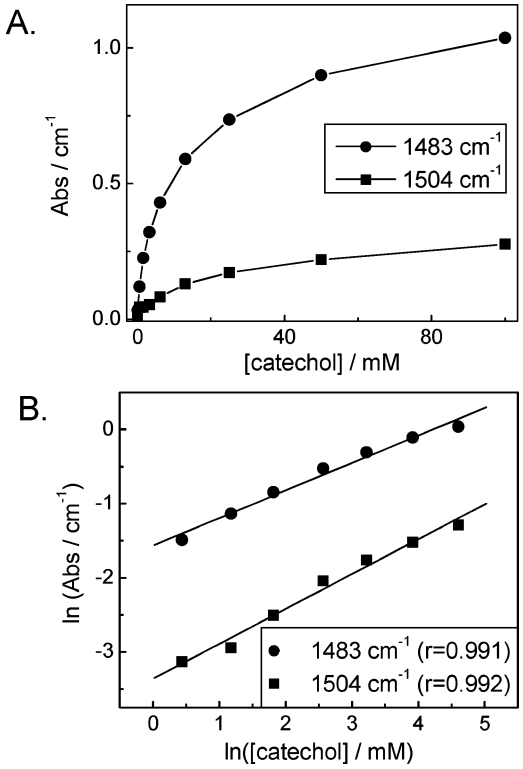

Figure 3. (A) Integrated absorbance for the deconvoluted bands at 1483 and 1504 cm^{-1} corresponding respectively to chelating and molecularly adsorbed catechol species at anatase nanoparticles in $HClO_4$ 0.1 M vs catechol concentration. (B) Logarithmic plot of the integrated absorbance for the bands at 1483 and 1504 cm^{-1} vs catechol concentration (Freundlich isotherm fitting).

3.3. Resonance Raman Spectroscopy. The infrared studies described above have evidenced the existence of two adsorbates. The most stable one has been assigned to a bidentate chelate adsorbing at Ti(4) surface sites. The second one would correspond to catechol molecularly adsorbed through van der Waals/hydrogen bonds with Ti(5) and O neighboring surface sites (see Scheme 1). One subject of special interest in heterogeneous photochemistry is that of photosensitization of wide band gap semiconductors. In the case of catechol adsorbed at TiO_2, Moser et al. demonstrated the formation of a charge-transfer complex for the first time.[9] Figure 4A shows UV/vis spectra for TiO_2 and TiO_2/catechol dispersions. As observed the modification with catechol extends the absorption of the

(44) Roddick-Lanzilotta, A. D.; Connor, P. A.; McQuillan, A. J. *Langmuir* **1998**, *14*, 6479.
(45) Morand, R.; Noworyta, K.; Augustynski, J. *Chem. Phys. Lett.* **2002**, *364*, 244.

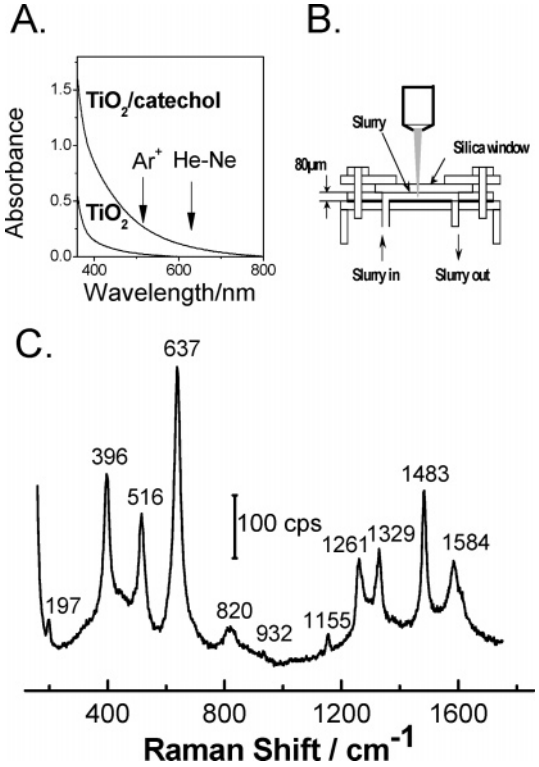

Figure 4. (A) UV−vis absorbance spectra for an anatase suspension in $HClO_4$ 0.1 M (both in the absence and in the presence of catechol 13 mM). (B) Sketch of the spectrochemical cell for the slurry analysis with the confocal microprobe Raman system. (C) Raman spectrum obtained for a TiO_2 slurry in contact with a 14.5 mM catechol + 0.1 M $HClO_4$ solution (acquisition time 20 s). The excitation line was provided by an Ar^+ laser (514.5 nm); grating of 1800 g/mm.

dispersion to the visible. This absorption onset shift is attributed to the formation of a catechol-to-anatase charge-transfer complex. Importantly here, there is absorption at the wavelengths of the laser excitation lines employed in the Raman experiments, which makes possible the existence of enhancement by resonance. It is critical to identify which of the two proposed adsorption configurations corresponds to the charge-transfer complex and gives rise to a significant redshift in the excitation energy of TiO_2. To this aim, the use of RRS is especially indicated because only the adsorbate forming the surface charge-transfer complex will be monitored as it will be the only absorbing incident laser radiation and giving rise to resonance enhancement. We followed the same approach in a preliminary study of the adsorption of salicylic and ascorbic acids on TiO_2.[29] Working in acidic media is recommended because Raman resonance for dissolved catechol species and the corresponding interference in adsorbate spectra are avoided this way.

As it will be shown in the following, illumination with the excitation laser beam induces the oxidative polymerization of adsorbed catechol, this process being much faster in the case of nanoporous thin films than in the case of slurries. We discuss first the RRS spectra for anatase suspensions in the presence of catechol because high-quality spectra can be obtained for the adsorbate prior to significant polymerization. RRS spectra for the nanoporous films will be discussed in section 3.4. Figure 4C corresponds to a Raman spectrum obtained for a concentrated suspension of anatase (slurry of 0.16 g cm^{-3}) in a 14.5 mM catechol + 0.1 M $HClO_4$ solution. The bands at 197, 396, 516, and 637 cm^{-1} correspond to lattice vibrations of the TiO_2 nanocrystals.[46] The band at 820 cm^{-1} appears in the spectra for the anatase nanopowders at a different frequency and with a lower intensity, both in air and in contact with an aqueous solution. In similar experiments done with salicylic and ascorbic acids, weaker bands also appear in this spectral region (but not at the same frequency).[29] On the other hand, no band is expected at this frequency for catechol species.[34,36,38] No firm assignment can be done at present, but it is tempting to ascribe it to a coupled plasmon-longitudinal optical-phonon mode.[47,48] The small band at 932 cm^{-1} is due to solution and interphasial ClO_4^-.

The bands corresponding to the resonance Raman spectrum for adsorbed catechol appear in the range 1150−1600 cm^{-1} (see Table 1). The strongest features are the ring stretch at 1483 cm^{-1} together with the C−O stretches (coupled with ring stretches) at 1261, 1329, and 1584 cm^{-1}.[28,36,38] In addition a less intense band appears at 1155 cm^{-1} associated to an in-plane CH bend.[28,36] Importantly, three of these bands appear at precisely the same frequencies in the infrared spectrum of the adsorbate. A similar spectrum is obtained if the excitation is provided by a He−Ne laser (at 632.8 nm). However, the intensity of the adsorbed catechol bands relative to that of dissolved perchlorate, which is not enhanced, is 5 to 9 times higher for the 514.5-nm laser than for the 632.8-nm laser, as expected for resonance Raman scattering.

It is interesting to compare the spectrum of adsorbed catechol with those found for catechol both in solid state and in solution (Figure 5). A first inspection of these spectra clearly indicates that the spectrum for the adsorbate resembles to some extent that found in alkaline solution where both catecholate species are present and is rather different from those obtained for solid state and for acidic solutions. However, the intense band at 1208 cm^{-1} mode appearing in the spectrum in alkaline solution and probably associated to a δ(OH) mode does not appear in the adsorbate spectrum. More conclusively, there is a close correspondence between the spectrum of the adsorbate and that of $(NH_4)_2[Ti(cat)_3]\cdot 2H_2O$ both in solid state and in aqueous solution. In such a complex, chelating catecholates are bound to the Ti(IV) central ion.[34] Therefore the adsorbed species being monitored by RRS should be the chelating catecholate dianion, which confirms the assignment done on the basis of infrared results. However, for the catechol concentration being used (14.5 mM), the second adsorbate (molecularly adsorbed catechol) should be present on the anatase surface but none of its characteristic features can be distinguished in the Raman spectrum. In particular, the intense bands appearing at 776 and 1041−1044 cm^{-1} in the spectra acquired both in solid state and in acidic solution[36] are absent in the spectrum of Figure 4C. As the only species whose Raman spectrum is enhanced by resonance are those forming the surface charge complex, we deduce that catecholate is such a species and not molecularly adsorbed catechol. In fact, recent calculations evidence that the dissociative adsorption of catechol at defect sites (Ti(4) sites) leads to a much larger red-shift in the TiO_2 excitation energy than molecular adsorption.[20]

It is remarkable that in the spectrum of Figure 4C the resonance enhancement particularly affects the band appearing

(46) Beattie, I. R.; Gilson, T. R. *Proc. R. Soc. London, Ser. A* **1968**, *307*, 407.
(47) Baumard, J. F.; Gervais, F. *Phys. Rev. B* **1977**, *15*, 2316.
(48) Krost, A.; Richter, W.; Zahn, D. R. T. *Appl. Surf. Sci.* **1992**, *56*−*58*, 691.

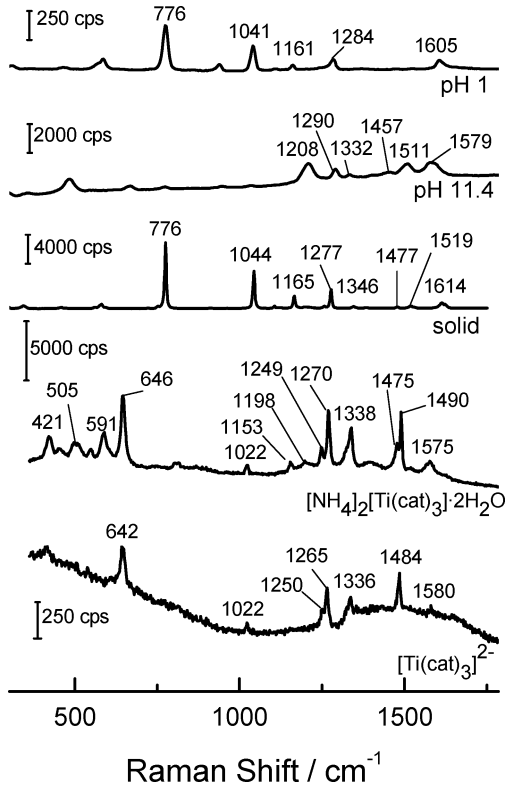

Figure 5. Raman spectra obtained for the following: a 1 M catechol solution of pH 1 (He−Ne laser; acquisition time 60 s, grating of 600 g/mm); a 1 M catechol solution of pH 11.4 (He−Ne laser, acquisition time 4 s, grating of 600 g/mm); solid catechol (Ar^+ laser, acquisition time 2.5 s, grating of 1800 g/mm); solid $(NH_4)_2[Ti(cat)_3]\cdot 2H_2O$ (diode laser at 784.8 nm, acquisition time 90 s, grating of 600 g/mm); and a saturated $(NH_4)_2[Ti(cat)_3]\cdot 2H_2O$ solution (diode laser at 784.8 nm, acquisition time 10 min, grating of 600 g/mm).

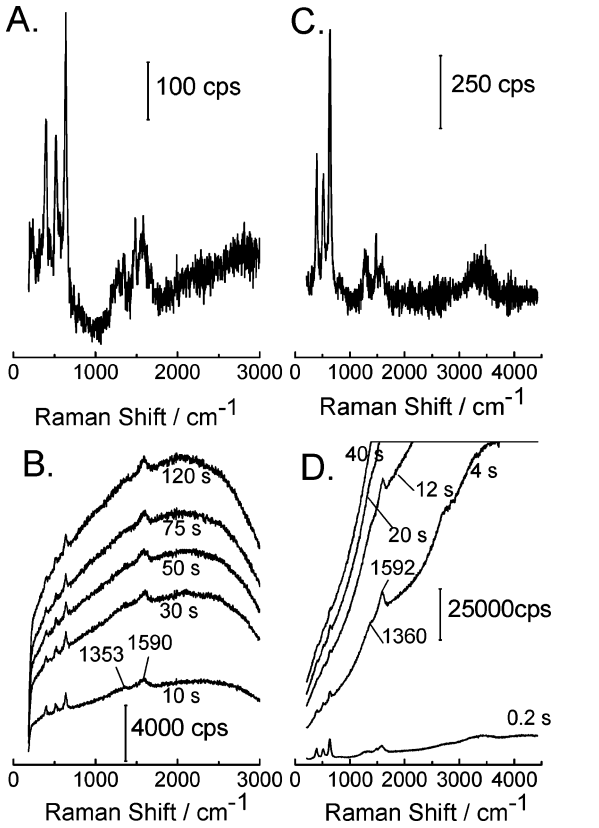

Figure 6. Raman spectra obtained for a nanoporous film of anatase on FTO conducting glass in contact with a 14.5 mM catechol + 0.1 M $HClO_4$ solution for different illumination times and different excitation lines: He−Ne laser (A and B) (acquisition time 0.5 s) and Ar^+ laser (C and D) (acquisition time 0.2 s). Experimental parameters: 600 μm pinhole; grating of 600 g/mm; 200 μm slit. Parts A and C correspond to the spectra collected at $t = 0$.

at 1329 cm^{-1}. According to Shoute and Loppnow, this can be considered as an indication that the catechol hydroxy groups provide the primary bridging adsorption bonds in keeping with the chelate adsorption geometry.[28] Finally, the appearance of strong features (Figure 4C) in the 1200−1600 cm^{-1} range suggests that the different modes involved are strongly coupled to the interfacial charge transfer. In other words, the charge transfer from adsorbed catechol to TiO_2 yields significant changes in geometry along the C−C, C−O, and ring vibrations. This is not unexpected since the π-molecular orbitals play a crucial role in electron injection.[15,19]

3.4. Reactivity under Illumination. The existence of charge transfer from adsorbed catechol to anatase nanoparticles opens up the possibility of light-induced interfacial reactivity. In fact, upon light absorption there is an almost instantaneous charge separation as demonstrated by femtosecond transient absorption spectrometry[18] and EPR.[17] While the electron is injected into the TiO_2 nanoparticle, the hole is localized in the adsorbed phase (catechol). Most of the electron−hole radical pairs recombine quickly (ps),[18,49] which, on the other hand, is responsible for the Raman resonance enhancement. However, some of the radical pairs are significantly stable (lifetime over 1 ms), which should facilitate that chemical processes could occur both in the adsorbed phase and in the surrounding solution. To check this, we studied the temporal evolution of the microRaman spectra for illumination with laser lines at 514.5 and 632.8 nm (Figure 6).

As observed, the well-defined bands characterizing the adsorbed molecule are transformed within seconds into less defined features centered at 1350−1360 and 1590−1600 cm^{-1}. Both of them can be attributed to ν(C═C) modes of aromatic rings with different degrees of substitution, although the contribution of dissociated carboxylates (symmetric and asymmetric stretches) cannot be discarded. Similar Raman spectra (and the corresponding assignments) have been reported for humic acids of different molecular weights.[50] It seems that, upon illumination, the catechol radical resulting from the electron injection into the TiO_2, which is probably an adsorbed *o*-benzosemiquinone,[17,51] initiates an oxidative polymerization process leading to a humic acid-type polymer. In fact, poly(catechol) has been considered as a model for this type of polymers.[52]

The Raman spectrum is not dominated however by vibrational bands, but for an increasing fluorescence, which could unfortunately obscure vibrational details of the species present at the surface upon illumination. However the existence of fluorescence, especially important when the 514.5 nm laser is being used, furnishes additional evidence for the photoinduced polymerization process. Decreasing the power of the incident laser

(49) Rajh, T.; Poluektov, O.; Dubinski, A. A.; Wiederrecht, G.; Thurnauer, M. C.; Trifunac, A. D. *Chem. Phys. Lett.* **2001**, *344*, 31.
(50) Francioso, O.; Sánchez-Cortés, S.; Casarini, D.; García-Ramos, J. V.; Ciavatta, C.; Gessa, C. *J. Mol. Struct.* **2002**, *609*, 137.
(51) Felix, C. C.; Sealy, R. C. *J. Am. Chem. Soc.* **1982**, *104*, 1555.
(52) Miano, T.; Sposito, G.; Martin, J. P. *Geoderma* **1990**, *47*, 349.

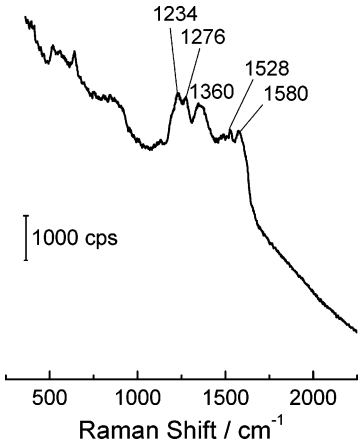

Figure 7. Raman spectrum obtained with a diode laser (784.8 nm) for a dried anatase thin film modified with the product resulting from catechol photopolymerization. Experimental parameters: 600 μm pinhole; grating of 600 g/mm; 200 μm slit; acquisition time 60 s.

probe by means of neutral density filters did not change the observed behavior. According to Miano et al., the synchronous-scan excitation spectrum ($\Delta\lambda = 18$ nm) for poly(catechol) shows an intense band at 498 nm, attributed to highly condensed ring structures, variously substituted. Thus, these structures are probably being formed during illumination with the laser probe. Interestingly, the polymerization of catechol can be heterogeneously catalyzed also upon adsorption on silver nanoparticles.[39,50,53]

Better-resolved Raman spectra can be obtained by using an excitation line of higher wavelength as, in this way, fluorescence is quenched. With this purpose, an anatase nanoporous thin film was immersed in a 14.5 mM catechol + 0.1 M $HClO_4$ solution and illuminated with an Ar^+ laser at 514.5 nm (110 mW) for 1 min. The illuminated spot became brownish in color because of the formation of a polymer layer attached to the TiO_2 thin film. Figure 7 shows the Raman spectrum obtained with a diode laser (784.8 nm) focused on the previously illuminated spot. Several bands may now be distinguished. The bands appearing between 1150 and 1300 cm^{-1} (a shoulder at 1190 cm^{-1} and bands at 1234 and 1276 cm^{-1}) are associated to C−O vibrations.[54] The broad one centered at approximately 1360 cm^{-1} can be attributed to ν(CC) modes of the aromatic rings without excluding the possibility of a contribution from the symmetric stretching vibration of carboxylates.[50] Finally, the bands in the region between 1450 and 1650 cm^{-1} are also typical of ν(CC) modes.[50,53,54] The polymeric nature of the substance formed upon illumination is evidenced especially by the shoulder at 1190 cm^{-1} and the band at 1276 cm^{-1} as they indicate the existence of ether C−O−C bonds between aromatic rings. In fact, Dubey et al.[54] performed the infrared characterization of poly(catechol) and attributed bands located at 1170 and 1280 cm^{-1} to the symmetric vibration of the (C−O−C) linkage present in the polymer and to this mode coupled to the C−OH vibration, respectively. Importantly, photopyrolysis (yielding graphite) provoked by high power laser illumination is not the main process induced by light at the SC/solution interface as the spectrum in Figure 7 differs significantly from the spectra

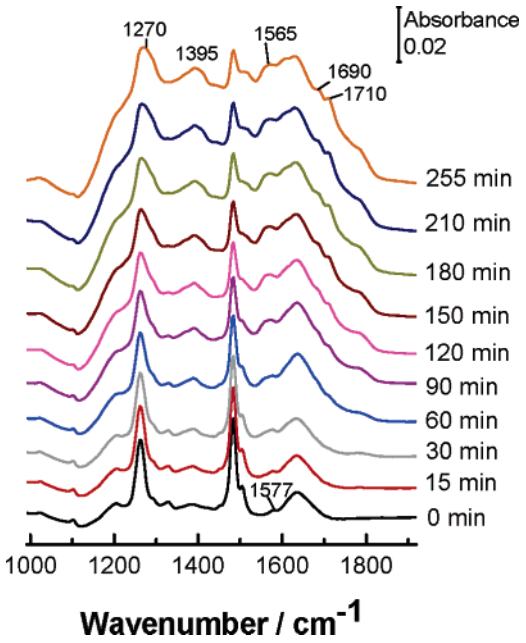

Figure 8. ATR-IR spectra obtained for a nanoporous film of anatase in contact with a 13 mM catechol + 0.1 M $HClO_4$ solution for different illumination times with a 50 W medium-pressure Hg lamp. The spectra were referred to a single beam spectrum collected in the absence of catechol.

typical of graphite with small size domains.[55] Therefore, upon illumination, the catechol radical resulting from the electron injection into the TiO_2 initiates a polymerization process. This radical remains anchored at the surface, which implies that in the end the resulting polymer is also attached to the surface as attested by Raman results and by the change in color of the illuminated samples. It is noteworthy that the photopolymerization in the visible is initiated by the adsorbed chelating catecholate rather than by molecularly adsorbed catechol, since the former is the one that becomes a radical upon injection of an electron into the TiO_2 nanoparticle. Once initiated, both adsorbed and dissolved catechol species are expected to participate in the polymerization process.

To further substantiate the light-induced oxidative condensation of catechol, infrared experiments were done under illumination from a 50 W mercury lamp (Figure 8). Again a broadening of the spectral features characterizing the adsorbate are observed together with the appearance of new ill-defined bands at 1270, 1395, 1565, 1690, and 1710 cm^{-1}. These bands are akin to those found in different samples of humic acids.[50,56] The band at 1270 can be assigned to a combination of the ν(C−O) of phenols and the asymmetric stretches of the C−O−C linkage.[54] The bands at 1395 and 1565 are probably due to the symmetric and asymmetric stretch of carboxylates, being the latter coupled to ν(C═C) modes of aromatic rings. Finally, the bands at 1690 and 1710 cm^{-1} are linked to ν(C═O) vibrations. Therefore the infrared results, in keeping with the Raman results, point to the condensation of catechol upon illumination giving rise to heterogeneous macromolecules similar to naturally found humic acids.

The formation of a humic acid-type polymer upon illumination with both visible and UV light has implications in the

(53) Sánchez-Cortés, S.; Francioso, O.; García-Ramos, J. V.; Ciavatta, C.; Gessa, C. *Colloids Surf. A* **2001**, *176*, 177.
(54) Dubey, S.; Singh, D.; Misra, R. A. *Enzyme Microb. Technol.* **1998**, *23*, 432.
(55) Nikiel, L.; Jagodzinski, P. W. *Carbon* **1993**, *31*, 1313.
(56) Alvarez, R.; Evans, L. A.; Milham, P. J.; Wilson, M. A. *Geoderma* **2004**, *118*, 245.

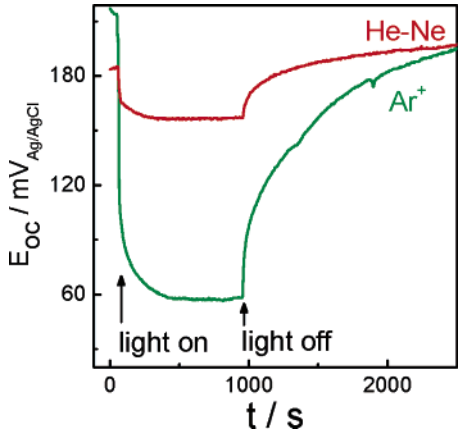

Figure 9. Open circuit potential variation for an anatase nanostructured electrode in contact with a 0.1 M $HClO_4$ + 14.5 mM catechol solution, under different illumination conditions: Ar^+ laser (6.1 mW) and He−Ne laser (5.8 mW). Illumination from the electrolyte side.

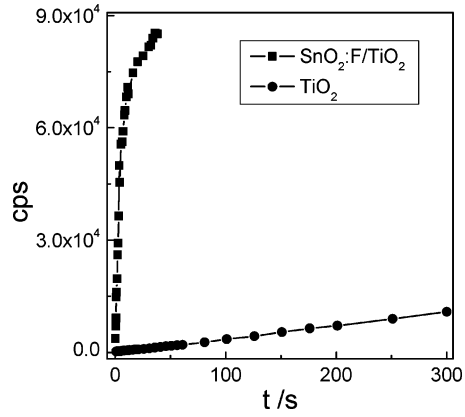

Figure 10. Time dependence of the fluorescence at 1000 cm^{-1} (excitation at 514.5 nm) obtained for a nanoporous film of anatase on FTO (3.5 μm thick) and for an anatase slurry (0.16 g cm^{-3}) in contact with a 14.5 mM catechol + 0.1 M $HClO_4$ solution.

practical use of anatase photocatalysts for water purification. First, for contaminants and reactants such as catechol, anatase is sensitized to visible light and through polymerization may be used for removing the contaminant from wastewater as the resulting polymer remains attached to the SC surface. Second, the polymerization process may lead to deactivation of the photocatalyst as evidenced very recently in the case of the heterogeneous oxidation of salicylic acid.[57]

The application of vibrational spectroscopies allows one to follow the changes occurring in the adsorbed phase due to the trapping of holes in it. However, little information can be deduced on the injection and delocalization of electrons within the TiO_2 nanostructured films. Evidence on this can be obtained through open circuit photopotential measurements, under experimental conditions that are tantamount to those used in the spectroscopic experiments. In the photopotential experiments what is actually measured is the change in the Fermi level of the F:SnO_2 substrate triggered by the illumination of the anatase nanostructured overlayer. This change is caused by the equilibration of the substrate Fermi level with the quasi-Fermi level of electrons in the nanostructured semiconductor. As the sole electronic states that communicate with the substrate are the extended ones,[58] the development of an open circuit photopotential responds to a photoinduced increase in the concentration of free electrons (electrons delocalized in the conduction band). Figure 9 shows the effect of illumination with laser lines at 632.8 and 514.5 nm on the open circuit potential (E_{oc}) for a nanostructured anatase thin film in contact with a deaerated 0.1 M $HClO_4$ + 14.5 mM catechol solution. As observed, upon illumination the open circuit potential drops and then attains a plateau (negative photopotential) as it corresponds to an accumulation of delocalized electrons in the conduction band. It is remarkable that even illumination at 632.8 nm causes injection into the conduction band. This indicates that there is a very broad distribution of electronic states for adsorbed catechol, and all of them (even those corresponding to the optical transition at the very end of the absorption tail) inject electrons into the conduction band. In agreement with our results, the delocalization of injected electrons upon TiO_2 sensitization with catechol has been suggested in both experimental[17,18,49] and theoretical studies.[19]

It is also remarkable that the recombination of electrons with the hole radicals in the adsorbed phase is a slow process as deduced from the slow decay of the photopotential once the illumination is interrupted. This is likely related to the delocalization of electrons through the nanoparticulate structure. On the other hand, this long-term stability (minutes) of the electron−hole radical pairs should be related to an increased chemical reactivity of the pairs. To test this, we performed parallel experiments on the temporal evolution of the Raman spectra both for an anatase thin film and a slurry and checked the emitted signal (fluorescence) at 1000 cm^{-1} (Figure 10). As observed, the emission signal grows almost linearly in both cases, but much faster (around 300 times) in the case of the thin film than for suspensions. As the fluorescence intensity is proportional to the number of fluorophore groups being sampled, it can be considered a relative measure of the amount of polymer formed. As the rate of a heterogeneous process is proportional to the interfacial area, we need to estimate the ratio of active area being sampled by the laser probe in both cases, *R*.

$$R = \frac{S_{film}}{S_{slurry}} \cong \frac{1}{2}\frac{N_{film}}{N_{slurry}} = \frac{1}{2}\frac{Adp/V_p}{Ahc_{anat}/m_p} = \frac{1}{2}\frac{dp\rho_{anat}}{hc_{anat}} \quad (1)$$

We assume that approximately 50% of the surface is lost in the film because of the sintering process and the tortuosity of the nanoporous channels, and therefore *R* is evaluated as half the ratio of the number of anatase nanoparticles (*N*) being sampled in each case. In eq 1, *A* corresponds to the area of the laser focal spot, *d*, to the film thickness, *p*, to the porosity of the film (anatase volume to total volume ratio), V_p and m_p, to the average nanoparticle volume and mass, ρ_{anat}, to the density of anatase (3.84 g cm^{-3}), *h*, to the effective height of the cylinder being sampled,[59] and c_{anat}, to the anatase concentration in the slurry (g cm^{-3}). In our particular experiments the film thickness is 3.5 μm, its porosity is assumed to be 0.5, and c_{anat} is 0.16 g cm^{-3}. The value of *h* depends on the pinhole size and the objective lens of the Raman instrument. For our instrument with a pinhole size of 600 μm and a 50× long working-length

(57) Franch, M. I.; Peral, J.; Domènech, X.; Ayllón, J. A. *Chem. Commun.* **2005**, 1851.

(58) Zaban, A.; Greenshtein, M.; Bisquert, J. *ChemPhysChem* **2003**, *4*, 859.

(59) Cai, W. B.; Ren, B.; Li, X. Q.; She, C. X.; Liu, F. M.; Cai, X. W.; Tian, Z. Q. *Surface Sci.* **1998**, *406*, 9.

objective (8 mm), *h* has been calculated to be 21 μm.[59] The resulting value for *R* is approximately 1. Therefore we can conclude that the heterogeneously photocatalyzed catechol condensation process is approximately 300 times faster in the case of the nanoporous film than for suspensions. Of course, this is a consequence of a lower recombination rate for the charge carriers in the case of the nanoporous film. Charge delocalization results in an increased distance between radical pairs. As mentioned above, the existence of a nanocrystal network makes possible the delocalization of the photogenerated electrons through the whole structure, whereas, in the case of the nanoparticle suspension, the electron can only delocalize within one particle or aggregate of particles.

4. Concluding Remarks

We have shown how to combine Raman and infrared spectroscopies together with photopotential measurements to study the adsorption and photoinduced reactivity for a typical system such as catechol adsorbed on anatase nanoparticles. This system can be considered as a model not only for photosensitization but also in photocatalysis. The combined approach employed here for the first time takes advantage of the complementarity of these experimental techniques. In fact, both spectroscopies provide vibrational information, but whereas ATR-IRS is characterized by a high sensitivity, Raman spectroscopy needs an enhancement mechanism to be sensitive to small amounts of substance such as those forming adsorbed layers. In our case, the enhancement is linked to resonance due to light absorption by the scattering species, and it is thus restricted to the species forming the surface charge complex, which allows for a high degree of specificity. The combination of sensitivity and selectivity furnished by the use of both vibrational spectroscopies can be further complemented with photoelectrochemical measurements (photopotential in this case), which provide macroscopic information on the photoinduced charge separation typical of the photosensitization and photocatalytic processes.

Our results show that catechol adsorbs on anatase nanoparticles from acidic aqueous solutions in two different coexisting configurations as suggested previously.[11] The most stable adsorbed species is bound to Ti four-fold coordinated surface sites as catecholate (fully dissociated), forming a chelate. The other adsorbate corresponds to a molecularly bound catechol species. Only the first species forms the charge-transfer complex responsible for sensitization to the visible, in keeping with theoretical calculations.[20]

We have also employed both vibrational spectroscopies to follow the photoinduced reactivity of this system. Irradiation of dispersions or thin films of anatase nanoparticles in contact with acidic aqueous solutions of catechol gives rise to a broadening of the original spectral features together with the appearance of new bands associated to processes of condensation and oxidation. In addition, an increasing fluorescence arises, which indicates the appearance of fluorophores in the resulting products, probably humic acid-type polymers. On the other hand, parallel photoelectrochemical experiments indicate the development of a negative photopotential resulting from the accumulation of free electrons in the conduction band of the semiconductor, which indicates not only electron injection into the semiconductor but also subsequent delocalization of the free charge. Interestingly this injection occurs even for illumination with 632.8-nm light. Scheme 2 summarizes the behavior of the system.

Scheme 2. Photoinduced Processes for the Catechol−TiO_2 System under Visible Illumination

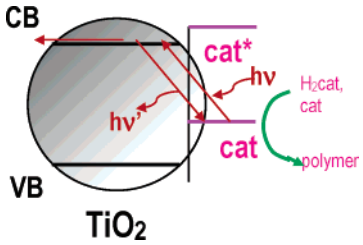

Evidence has been given for the different behaviors of dispersions and thin films of anatase nanoparticles. The catechol apparent adsorption free energies found here for thin films are significantly lower than values reported for anatase dispersions.[9,11,13] As suggested previously in connection with quartz microbalance measurements, we believe that this difference is most probably linked to the hydrophobicity imparted by the adsorbate to the pores of the thin film. In addition the kinetics of fluorescence development is much faster in the case of the thin film, indicating a higher reactivity. Most probably, this behavior is linked to an increased distance between photogenerated radical pairs caused by electron delocalization through the three-dimensional nanocrystalline structure. This delocalization is much less effective in nanoparticle dispersions, even if aggregation occurs. On the basis of these effects we may anticipate that the reactivity of nanoporous layers may differ considerably from that of the corresponding colloidal dispersions, which is relevant to photoelectrochemical and photocatalytic applications.

Acknowledgment. The Spanish Ministerio de Educación y Ciencia and the Generalitat Valenciana are acknowledged for financial support through Project Nos. BQU2003-03737 (Fondos FEDER) and GV05/119, respectively. T.L.V. is grateful to the MEC (Spain) for the award of a FPU grant. We also thank the SS.TT.II. and the Vice-presidency of Research of the University of Alicante.

Supporting Information Available: Table showing the relative intensity of the adsorbate Raman bands as a function of the exciting wavelength and figure showing the effect of the exciting light intensity on the temporal evolution of the adsorbate Raman spectra. This material is available free of charge via the Internet at http://pubs.acs.org.

JA052798Y